Ultrafast modulation of optical metamaterials

David J. Cho,[1] Wei Wu,[2] Ekaterina Ponizovskaya,[2] Pratik Chaturvedi,[2] Alexander M. Bratkovsky,[2] Shih-Yuan Wang,[2] Xiang Zhang,[3, 4] Feng Wang,[1, 4] and Y. Ron Shen[1, 4]*

[1]*Department of Physics, University of California at Berkeley, Berkeley, California 94720, USA*
[2]*Information and Quantum Systems Lab, Hewlett-Packard Laboratories, Palo Alto, California 94304, USA*
[3]*5130 Etcheverry Hall, Nanoscale Science and Engineering Center, University of California at Berkeley, Berkeley, California94720, USA*
[4]*Materials Science Division, Lawrence Berkeley National Laboratory, Berkeley, California 97420, USA*
**yrshen@berkeley.edu*

Abstract: We show by pump-probe spectroscopy that the optical response of a fishnet metamaterial can be modulated on the femtosecond time scale. The modulation dynamics is dominated by pump-induced changes in the constituting dielectric medium, but the strength of modulation is dramatically enhanced through the plasmon resonance. The pump-induced spectral responses of the metamaterial provide understanding on how the resonance is modified by pump excitation. Our study suggests that metamaterials can be used as high-speed amplitude/phase modulators with terahertz-bandwidth.

OCIS codes: (160.3918) Metamaterials; (240.6680) Surface plasmons; (240.6380) Spectroscopy, modulation.

References and links

1. V. M. Shalaev, "Optical negative-index metamaterials," Nat. Photonics **1**(1), 41–48 (2007).
2. C. M. Soukoulis, S. Linden, and M. Wegener, "Physics. Negative refractive index at optical wavelengths," Science **315**(5808), 47–49 (2007).
3. N. Fang, H. Lee, C. Sun, and X. Zhang, "Sub-diffraction-limited optical imaging with a silver superlens," Science **308**(5721), 534–537 (2005).
4. J. B. Pendry, D. Schurig, and D. R. Smith, "Controlling electromagnetic fields," Science **312**(5781), 1780–1782 (2006).
5. E. Kim, Y. R. Shen, W. Wu, E. Ponizovskaya, Z. Yu, A. M. Bratkovsky, S. Y. Wang, and R. S. Williams, "Modulation of negative index metamaterials in the near-IR range," Appl. Phys. Lett. **91**, 3 (2007).
6. H. T. Chen, W. J. Padilla, M. J. Cich, A. K. Azad, R. D. Averitt, and A. J. Taylor, "A metamaterial solid-state terahertz phase modulator," Nat. Photonics **3**(3), 148–151 (2009).
7. S. Zhang, W. J. Fan, K. J. Malloy, S. R. J. Brueck, N. C. Panoiu, and R. M. Osgood, "Near-infrared double negative metamaterials," Opt. Express **13**(13), 4922–4930 (2005).
8. W. Wu, E. Kim, E. Ponizovskaya, Y. Liu, Z. Yu, N. Fang, Y. R. Shen, A. M. Bratkovsky, W. Tong, C. Sun, X. Zhang, S. Y. Wang, and R. S. Williams, "Optical metamaterials at near and mid-IR range fabricated by nanoimprint lithography," Appl. Phys., A Mater. Sci. Process. **87**(2), 143–150 (2007).
9. A. Taflove, and S. Hagness, *Comupational Electrodynamics: The Finite-Difference Time-Domain Method* (Artech House, 2005).
10. W. Wu, E. Ponizovskaya, E. Kim, D. Cho, A. Bratkovsky, Z. N. Yu, Q. F. Xia, X. M. Li, Y. R. Shen, S. Y. Wang, and R. S. Williams, "Geometrical dependence of optical negative index meta-materials at 1.55 mu," Appl. Phys., A Mater. Sci. Process. **95**(4), 1119–1122 (2009).
11. M. Born, and E. Wolf, *Principle of Optics* (Cambridge University Press, 1999).
12. A. V. Kildishev, W. S. Cai, U. K. Chettiar, H. K. Yuan, A. K. Sarychev, V. P. Drachev, and V. M. Shalaev, "Negative refractive index in optics of metal-dielectric composites," J. Opt. Soc. Am. B **23**(3), 423–433 (2006).
13. D. R. Smith, S. Schultz, P. Markos, and C. M. Soukoulis, "Determination of effective permittivity and permeability of metamaterials from reflection and transmission coefficients," Phys. Rev. B **65**(19), 195104 (2002).
14. D. J. Cho, F. Wang, X. Zhang, and Y. R. Shen, "Contribution of the electric quadrupole resonance in optical metamaterials," Phys. Rev. B **78**(12), 121101 (2008).
15. A. Esser, K. Seibert, H. Kurz, G. N. Parsons, C. Wang, B. N. Davidson, G. Lucovsky, and R. J. Nemanich, "Ultrafast Recombination and Trapping in Amorphous-Silicon," Phys. Rev. B **41**(5), 2879–2884 (1990).
16. E. S. Harmon, M. R. Melloch, J. M. Woodall, D. D. Nolte, N. Otsuka, and C. L. Chang, "Carrier Lifetime Versus Anneal in Low-Temperature Growth Gaas," Appl. Phys. Lett. **63**(16), 2248–2250 (1993).

#115620 - $15.00 USD Received 13 Aug 2009; revised 12 Sep 2009; accepted 13 Sep 2009; published 17 Sep 2009

17. C. Carmody, H. H. Tan, C. Jagadish, A. Gaarder, and S. Marcinkevicius, "Ultrafast carrier trapping and recombination in highly resistive ion implanted InP," J. Appl. Phys. **94**(2), 1074–1078 (2003).
18. M. Kubinyi, A. Grofcsik, and W. J. Jones, "Laser spectroscopic study of photoinduced picosecond processes in amorphous and polycrystalline silicon films," (Elsevier Science Bv, 1997), pp. 121–124.

Optical metamaterials have attracted immense interest in recent years [1,2] because they could lead to novel phenomena and applications such as sub-diffraction imaging [3] and cloaking [4]. Active control of their properties could further facilitate and open up new applications in terms of modulation and switching [5,6]. It is therefore important to know the dynamic response of metamaterials to an external perturbation and understand the underlying physical mechanism.

Here we report the spectral and dynamic behavior of optical modulation in a metamaterial with the "fishnet" structure [7]. Using femtosecond pump-probe spectroscopy with an interferometer, we measured the pump-induced spectral changes of transmission, reflection and their phases over the magnetic plasmon resonance of the fishnet. We observed for the first time that the induced change had a fast relaxation time of ~750fs, and the magnitude of change was dramatically enhanced compared to that in natural materials. The spectral changes indicated that the effect mainly came from pump-induced broadening of the resonance. The results suggest that further improvement of the modulation characteristics is possible with better choice of the dielectric material in the fishnet structure.

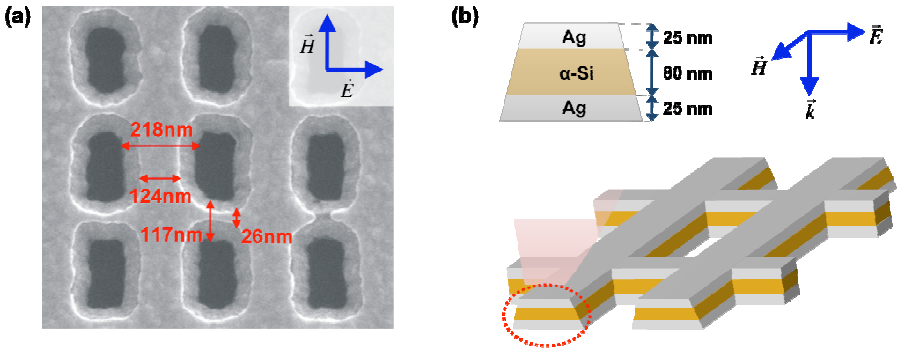

Fig. 1. Fishnet structure (a) SEM image of a sample. Its grid-like structure is composed of thin wires (top: 26nm, bottom: 117nm) and thick wires (top: 124nm, bottom: 218nm) orthogonal to each other. Inset shows the polarizations of the electric field ($\vec{E}$) and magnetic field ($\vec{H}$) of incident light. (b) Schematic of the fishnet showing the thicknesses of the Ag(25nm)/ *a*-Si (80nm)/Ag(25nm) sandwiched layers. The tapered sidewall results from the fabrication process.

The fishnet structure we studied is described in Fig. 1 with a scanning electron microscope (SEM) image (Fig. 1(a)) and a schematic of its three dimensional structure (Fig. 1(b)). The fishnet was prepared by nanoimprint lithography [8] and composed of Ag(25nm)/*a*-Si(80nm)/Ag(25nm) sandwiched layers on a silica substrate. It was designed using the finite-difference-time-domain (FDTD) method [9] to have a magnetic response in the near-infrared. Adjusting the width and thicknesses of the grids along with selecting material of proper dielectric constants allows fine tuning of the resonant frequency to the desired value [10]. We measured the complex transmission ($\hat{t} = |\hat{t}| e^{i\phi_t}$) and reflection ($\hat{r} = |\hat{r}| e^{i\phi_r}$) coefficients of the fishnet, with and without pump, using the setup depicted in Fig. 2 which implements a Michelson-type interferometer arrangement for absolute phase measurement. A 20-MHz super-continuum fiber laser providing 5ps pulses with wavelength covering from 450 to 2000nm was employed to probe the sample without pump. For the pump-probe studies, 100-fs pulses at 800 nm from a 1-kHz Ti:Sapphire laser were used as the pump and tunable near-infrared pulses (1.05-3.3μm) generated from the laser-pumped optical parametric amplifier (OPA) system used as the probe.

#115620 - $15.00 USD Received 13 Aug 2009; revised 12 Sep 2009; accepted 13 Sep 2009; published 17 Sep 2009

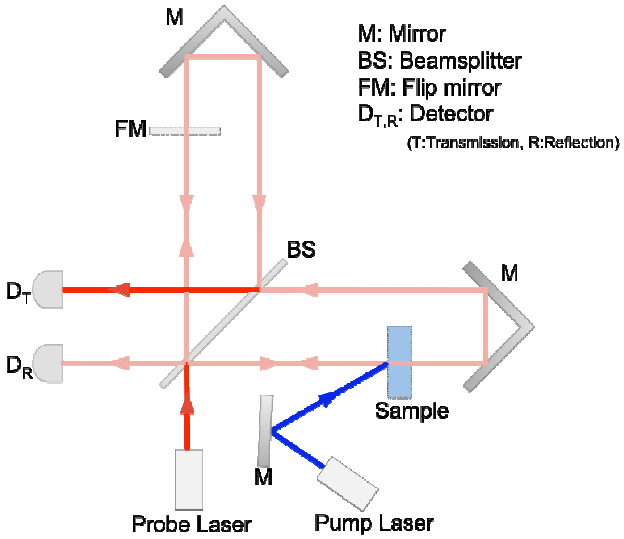

Fig. 2. Experimental setup to measure T = $|\hat{t}|^2$, R = $|\hat{r}|^2$, ϕ_t and ϕ_r of the complex transmission ($\hat{t}$) and reflection ($\hat{r}$) coefficients. A Michelson-type interferometer is implemented for absolute phase measurement. The near-infrared tunable probe pulses come from a super-continuum fiber laser and an OPA system, respectively, for measurements without and with pump. The pump pulses at 800 nm are from a 1-kHz Ti:Sapphire laser. The pump-probe time delay is adjusted by a motorized mirror stage (not shown). The flip mirror is used as a reference for reflection measurements.

From the measured $\hat{t}$ and $\hat{r}$, we could deduce the complex effective refractive index ($\hat{n}$) and impedance ($\hat{z}$) using the following relations [11,12],

$$\hat{n} = \frac{1}{k_o d}\cos^{-1}\left[\frac{1-\hat{r}^2+n_s\hat{t}^2}{(n_s+1)\hat{t}+\hat{r}\hat{t}(n_s-1)}\right] \tag{1a}$$

and

$$\hat{z} = X \pm \sqrt{X^2+\frac{1}{n_s}} \tag{1b}$$

where $X = \frac{i}{2n_s \sin(\hat{n}k_o d)}\left[\frac{2\hat{r}}{\hat{t}}+(n_s-1)\cos(\hat{n}k_o d)\right]$.

Here, k_o is the wavevector in free space, d is the thickness of the metamaterial and n_s is the refractive index of the substrate. The proper sign in $\hat{z}$ is chosen by satisfying the conditions $\mathrm{Im}(\hat{n}) > 0$ and $\mathrm{Re}(\hat{z}) > 0$ for passive materials [13]. The effective permittivity ($\hat{\varepsilon}$) and permeability ($\hat{\mu}$) can be obtained from $\hat{\varepsilon} = \hat{n}/\hat{z}$ and $\hat{\mu} = \hat{n}\hat{z}$. The asymmetry of the tapered layers on the light illumination direction has to be considered for a more accurate description. Here, we ignore this factor and use the standard retrieval method because the effect is small for thin films.

#115620 - $15.00 USD Received 13 Aug 2009; revised 12 Sep 2009; accepted 13 Sep 2009; published 17 Sep 2009

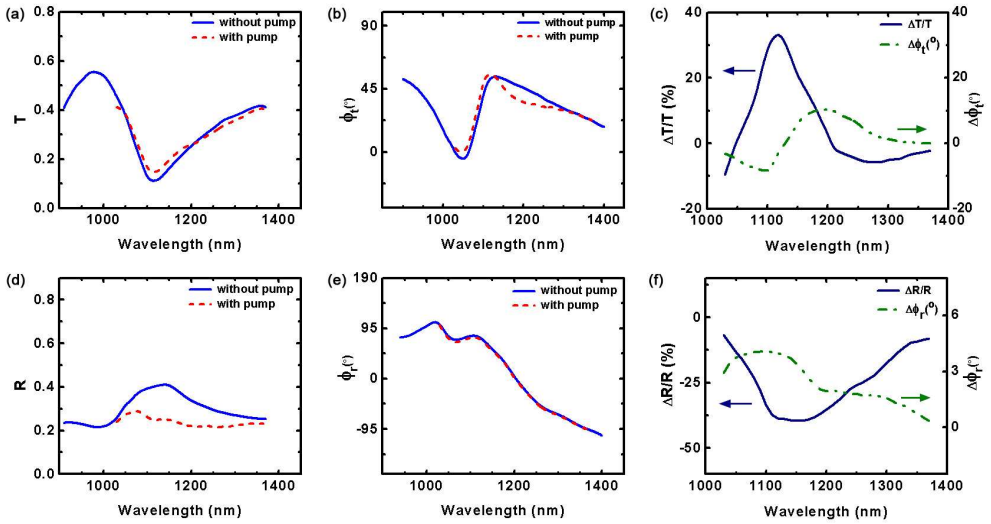

Fig. 3. Experimentally measured spectra of T, R, ϕ_t and ϕ_r with and without pump. (a) T. (b) ϕ_t. (c) ΔT/T and $\Delta\phi_t$. (d) R. (e) ϕ_r. (f) ΔR/R and $\Delta\phi_r$. The pump-induced changes ΔT/T, ΔR/R, $\Delta\phi_t$ and $\Delta\phi_r$ were directly measured and added to the blue solid curves of (a,b,d,e) to obtain the corresponding red dashed curves for the case with pump (300μJ/cm^2).

A complete characterization of the fishnet metamaterial is shown in Fig. 3. Blue solid lines in Fig. 3(a,b,d,e) display the measured $T=|\hat{t}|^2$, $R=|\hat{r}|^2$, ϕ_t, and ϕ_r, respectively. The pump-induced changes of ΔT/T, ΔR/R, $\Delta\phi_t$ and $\Delta\phi_r$ at pump fluence of 300μJ/cm^2 and probe fluence of ~0.5μJ/cm^2 were measured using a lock-in technique, and the results are plotted in Fig. 3(c) and 3(f). Transmission and reflection parameters with pump on were obtained by adding the pump-induced changes to metamaterial linear responses, which are shown as red dashed lines in Fig. 3(a,b,d,e). The effective $\hat{n}$, $\hat{\varepsilon}$, $\hat{\mu}$ and their modulations can be deduced readily and the results are plotted in Fig. 4. The magnetic resonance with the characteristic resonant spectral features (e.g., dip in T and peak in R) around 1.15μm (which is the resonant wavelength defined by the peak of $\mathrm{Im}(\hat{\mu})$) clearly exists in all curves. The pump-induced spectral changes of all quantities around the resonance are also clearly observed. The distinct resonant features of $\hat{\mu}$ confirm a strong magnetic resonance. We note that $\mathrm{Re}(\hat{\varepsilon})$ also exhibits spectral features at the magnetic resonance, indicating that the resonance is not purely magnetic, a result arising from the tapered layer structure of the fishnet [10] (Fig. 1(b)) that causes mixing of the usual symmetric and asymmetric resonant modes [14]. As expected, the pump-induced change is most appreciable near resonance. With the probe wavelength at 1.12μm, we observed changes of ΔT/T = 31% and ΔR/R = −42% for a pump fluence of 300μJ/cm^2 at zero pump-probe time delay. The changes are linear with pump fluence as shown in Fig. 5(a). The different signs of ΔT and ΔR are the result of a decrease in $\mathrm{Im}(\hat{n})$ (which mainly follows from decrease of $\mathrm{Im}(\hat{\mu})$) at the magnetic resonance (Fig. 4(b) and 4(f)). When we used the same pump on an *a*-Si film with the same thickness (80nm) as that in the fishnet structure, the observed ΔT/T and ΔR/R were both less than 1%. Thus, the pump-induced changes of ΔT/T and ΔR/R in the fishnet appear to be larger than 50 times. This dramatic enhancement comes from enhancement through the plasmon resonance: a small change in the refractive index of the dielectric layer in the fishnet can induce a significant change in the plasmon resonant characteristics, and hence the optical properties of the fishnet near resonance. Thus, metamaterials can be a very effective optical modulator.

#115620 - $15.00 USD Received 13 Aug 2009; revised 12 Sep 2009; accepted 13 Sep 2009; published 17 Sep 2009

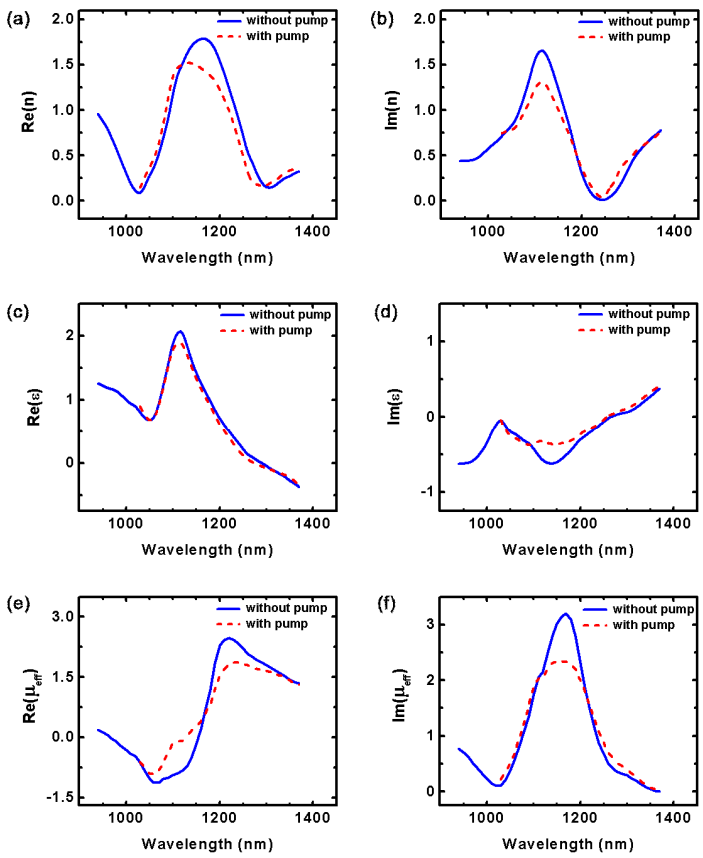

Fig. 4. Experimentally deduced $\hat{n}$, $\hat{\varepsilon}$ and $\hat{\mu}$ from $\hat{t}$ and $\hat{r}$ with and without pump. (a) Re($\hat{n}$). (b) Im($\hat{n}$). (c) Re($\hat{\varepsilon}$). (d) Im($\hat{\varepsilon}$). (e) Re($\hat{\mu}$). (f) Im($\hat{\mu}$). The blue solid and red dash curves are deduced from those of (a,b,d,e) of Fig. 2 using Eq. (1).

We also measured relaxation of ΔT/T and ΔR/R after pumping and deduce relaxation of the pump-induced absorption change (ΔA) for both the fishnet and the *a*-Si film. The pump fluence used was 300μJ/cm^2. As shown in Fig. 5(b), the pump-induced absorptions in the two cases are similar. The induced changes as function of probe-pump time delay have a fast decay component of ~750fs followed by a long tail extending over hundred picoseconds. We note that differently prepared *a*-Si can have different relaxation dynamics [15]. The similar decay dynamics of *a*-Si and the fishnet incorporating it indicate that the fishnet modulation dynamics is dominated by free carrier excitation in *a*-Si and the contribution from excited carriers in the metal layers is negligible. This is reasonable because the maximum excited carrier density in the silver layer estimated from the pump fluence is ~10^{18}cm^{-3}, which is orders of magnitude smaller than the intrinsic free carrier density ~10^{23}cm^{-3}, and therefore its effect on the optical properties of the fishnet is not significant. Thus, for better pump-induced modulation strength and speed, we need to choose dielectric materials with stronger absorption coefficient and shorter carrier lifetime for the fishnet. For example, low-temperature grown GaAs is known to have carrier lifetimes of ~200fs [16] and so is ion-implanted InP [17]. Both have strong direct interband absorption that can lead to large modulation depth with lower pump fluence.

#115620 - $15.00 USD Received 13 Aug 2009; revised 12 Sep 2009; accepted 13 Sep 2009; published 17 Sep 2009

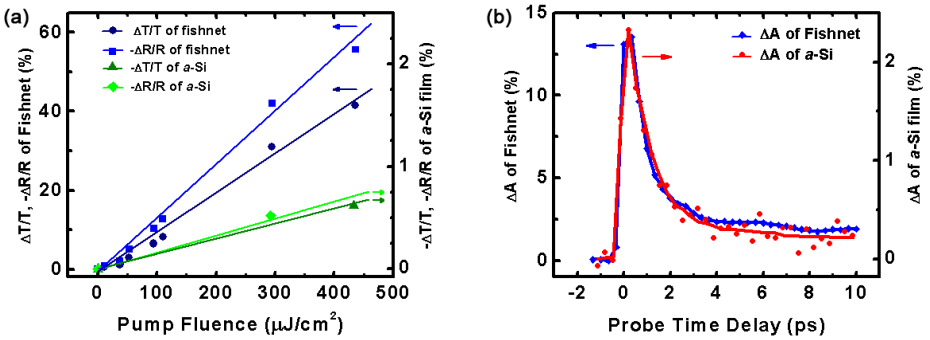

Fig. 5. Pump-induced responses of the fishnet and *a*-Si film. (a) Normalized changes of transmission and reflection versus pump fluence. (b) Pump-induced absorptions versus probe-pump time delay. Note the different scales for fishnet and *a*-Si film.

It is observed that the pump-induced changes come in mainly through broadening of the magnetic resonance (seen in the spectra of $\hat{\mu}$ in Fig. 4(e) and 4(f)), and should result from the induced refractive index changes, Δn^{f} and Δk^{f}, of *a*-Si in fishnet. These can be estimated from the refractive index change, Δn^{b} and Δk^{b}, of the bare *a*-Si film, which are deduced from the measured changes of transmittivity (T^{b}) and reflectivity (R^{b}) of the film using the relations [18],

$$\Delta \mathrm{T}^{\mathrm{b}} = (\frac{\partial \mathrm{T}^{\mathrm{b}}}{\partial n^{\mathrm{b}}})\Delta n^{\mathrm{b}} + (\frac{\partial \mathrm{T}^{\mathrm{b}}}{\partial k^{\mathrm{b}}})\Delta k^{\mathrm{b}} \quad \text{and} \quad \Delta \mathrm{R}^{\mathrm{b}} = (\frac{\partial \mathrm{R}^{\mathrm{b}}}{\partial n^{\mathrm{b}}})\Delta n^{\mathrm{b}} + (\frac{\partial \mathrm{R}^{\mathrm{b}}}{\partial k^{\mathrm{b}}})\Delta k^{\mathrm{b}}. \qquad (2)$$

We obtained $\Delta n^{\mathrm{b}} = -0.01$ and $\Delta k^{\mathrm{b}} = 0.05$. Δn^{f} and Δk^{f}, being similar to these values, are mainly responsible for the shift and broadening of the magnetic resonance, respectively. In our case, the shift of resonance is not appreciable, and only the effect of Δk^{f} is significant. In general, however, one could use both Δn^{f} and Δk^{f} to shift and broaden the resonance to achieve strong modulation. Large Δn^{f} alone could be obtained in dielectric materials such as liquid crystals and polyelectrolytes.

Interestingly, we notice that Fig. 3(c) show correlations between pump-induced changes of different quantities. The maximum ΔT occurs around minimum $\Delta\phi_t$ and vise versa, at 1.12μm and 1.2μm, respectively. This can be readily understood knowing that the pump-induced changes of Re($\hat{n}$) and Im($\hat{n}$) are correlated, and as can be seen from Eq. (1), ΔT and $\Delta\phi_t$ depends much more strongly on Im($\hat{n}$) and Re($\hat{n}$), respectively. Thus, both amplitude and phase modulations are achievable and can be predicted from understanding of how the optical constants behave under external perturbation.

In summary, we have demonstrated ultrafast pump-induced optical modulation in a fishnet metamaterial. The modulation was governed by the properties of the dielectric layer in the fishnet. Its relaxation time corresponded to the excited carrier lifetime of the dielectric medium, and its strength was determined mainly by the induced imaginary refractive index change in the dielectric. The results indicate that stronger and faster modulation could be achieved by proper choice of the dielectric in the structure of the metamaterial.

Acknowledgments

This work was supported by DARPA and NSF Nanoscale Science and Engineering Center (NSEC) under Grant No. DMI-0327077.

#115620 - $15.00 USD Received 13 Aug 2009; revised 12 Sep 2009; accepted 13 Sep 2009; published 17 Sep 2009